ELSEVIER

Journal of Crystal Growth 211 (2000) 480–484

JOURNAL OF CRYSTAL GROWTH

www.elsevier.nl/locate/jcrysgro

Seeded growth from flux and neutron study of $La_{1-x}Ba_xMnO_3$ ($0.2 < x < 0.5$) single crystals

S.N. Barilo[a], G.L. Bychkov[a,*], L.A. Kurnevich[a], S.V. Shiryaev[a], L.A. Kurochkin[a], J.W. Lynn[b,c], L. Vasiliu-Doloc[b,c]

[a]*Institute of Solid State and Semiconductors Physics, Academy of Sciences, Minsk 220072, Byelorussia*
[b]*NIST Center for Neutron Research, Gaithersburg, MD 20899, USA*
[c]*Center for Superconductivity Research, University of Maryland, College Park, MD 20742, USA*

Abstract

The flux technique for growing large crystals of $La_{1-x}Ba_xMnO_3 (0.2 < x < 0.5)$ with a seed is discussed. Based on up to 40 wt% solubility of the solute, good rheological properties of corresponding flux melts, and desirable Ba substitution, the 25–40 mol% B_2O_3/45–60 mol% BaO/15–30 mol% BaF_2 range of solvents has been selected to grow crystals up to 1.5 cm^3 in volume. The best crystals have been grown under constant or a very slow increase of temperature in the interval 950–1250°C. Crystals with rocking curves of $\sim 0.3^\circ$ FWHM have been obtained. Layer-by-layer X-ray fluorescent analysis has confirmed a high homogeneity of Ba distribution in volume. Neutron triple-axis measurements have been done to study the spin dynamics of the $La_{0.68}Ba_{0.32}MnO_3$ crystal. Resistivity and AC-susceptibility results show that the peak occurs at a temperature T_p well above T_c (= 336 K). The data support the assumption that charge ordering exists to pin carriers.

PACS: 81.10. − h; 81.10.Dn; 75.30.Ds; 75.30.Vn

Keywords: Lanthanum–barium manganese oxide; Flux growth; Magnetoresistance; Spin wave spectra

1. Introduction

The perovskite-type of the doped $La_{1-x}M_xMnO_3$ class of materials with M = Ba, Sr, Ca, and Pb has attracted renewed interest because of the dramatic increase in conductivity these systems exhibit when the magnetic moments order ferromagnetically, either by temperature lowering or applying of a magnetic field [1]. This huge increase in the carrier mobility, which has been given the name "colossal magnetoresistivity" (CMR) [2], is both of scientific and technological interest. In particular, it is anticipated that these materials may provide the next generation of read/write heads for the data storage industry, while the "half-metallic" behavior provides fully spin-polarized electrons for use in magneto-electronics applications, and for sensors in a variety of devices of the automotive industry. According to experimental data about three orders of magnitude difference in electrical resistivity [2] and a discrepancy of thermal conductivity results [3] exist

* Corresponding author: Tel.: + 375-172-841-162; fax: + 375-172-840-888.
E-mail address: bars@ifttp.bas-net.by (G.L. Bychkov)

0022-0248/00/$ - see front matter
PII: S0022-0248(99)00767-8

between ceramic samples and single crystalline films. One should conclude that transport properties of doped manganese oxides are extremely sensitive to grain boundaries. Since the study of CMR manganites has great impact on both the basic understanding of the mechanism governing this phenomenon and the potential applications, high-quality single crystals are needed.

Single crystals of doped rare earth manganese oxides were obtained mainly by spontaneous crystallization from different fluxes [3–5] or using the floating zone method [6–8]. Both techniques exhibit definite advantages (disadvantages) when compared. Indeed, flux grown crystals demonstrated good homogeneity of the main ligand distribution in moderate volumes up to 150 mm^3 and a small mosaic spread of the lattice. However, cation substitution both in rare earth and manganese sites of CMR crystals grown from all solutions used so far is still a serious problem, which restricts the set of compositions that can be grown to Pb, Ba and alkali ion (Na, Li) doped compounds. Unfortunately, the lowest content of divalent ions in crystals grown from flux reached by alkali earth compounds is restricted by 20 mol%. The floating zone technique provides about several cm^3 in volume of manganite crystals, which differ by a small mosaicity in a whole range of solid solutions. Nevertheless, for the growth method a segregation problem still exists as well as manganese non-stoichiometry makes CMR crystal quality worse due to Mn evaporation from the melt.

In this paper we report the growth technique of large crystals of $La_{1-x}Ba_xMnO_3$ with a seed in the dynamic regime, from a flux based on B_2O_3–BaO–BaF_2 ternary system as a solvent. Neutron triple-axis measurements of the crystal spin dynamics combined with electrical resistivity and AC-susceptibility data are discussed.

2. Experimental procedure

Seeded growth of $La_{1-x}Ba_xMnO_3$ single crystals was carried out in a vertical furnace provided with SiC heaters. The home remade RIF-101 temperature controller allows one to stabilize temperature with an accuracy $\pm 0.1^{\circ}C$ as well as providing a temperature scan capability with a rate as small as $0.1^{\circ}C$/day with up to 30 days duration of growth. The flux melt was prepared by successive melting of 99.99% purity starting components individually weighed in molar ratio as presented in Table 1. Lanthanum oxide was annealed for 24 h at $1200^{\circ}C$ before weighing to avoid a considerable wetting of a platinum crucible by the flux. Having determined the saturation (T_{sat}) and spontaneous crystallization (T_{sp}) temperatures, separate crystals were allowed to grow up to a size of 1 mm^3 at temperature 1–$2^{\circ}C$ lower than T_{sp}. After thorough visual examination of facets, high-quality crystals were fixed on shields and mounted on a Pt crystal holder to be used as seeds. The temperature regime was determined by the consideration of rheological

Table 1
The data of $La_{1-x}Ba_xMnO_3$ ($0.2 < x < 0.5$) crystal growth experiment under conditions of B_2O_3–BaO–BaF_2 based flux melt evaporation

Run number	Flux melt composition (mol %)				La_2O_3 excess x (wt%)	Temperature sweep range (°C)	Seeds number	Growth time (days)	Ba content
	B_2O_3	BaO	BaF_2	$La_{1+x}MnO_3$					
15	46.51	17.12	36.37	14.68	80	1266	—	—	0.23
16	45.51	16.76	37.73	14.41	80	1255–1270	6	32	0.26
23	57.53	13.94	29.53	8.05	40	1186–1209	4	30	0.30
5	52.34	19.30	28.30	5.06	43.7	1146–1163	5	25	0.34
20	46.99	26.40	26.61	4.74	70	950–951	5	32	0.365
19	47.99	25.75	26.26	4.82	70	955	—	—	0.43

properties of the flux melt, concentration of the solute, the number of seeds, and the flux geometry in a growth run. Selected data of growth experiments are collected in Table 1. As can be seen Ba content in the crystals decreases with an increase in the growth temperature. The best crystals of $La_{1-x}Ba_xMnO_3$ up to 1.5 cm^3 in volume have been grown under the rate 0.1°C/day of temperature sweep, in the range $T_{sat} - 5°C < T < T_{sat}$ at the primary crystallization temperature interval 950–1250°C, to reveal $\sim 0.3°$ FWHM of neutron. The growth temperature was chosen separately depending on barium content $0.2 < x < 0.5$ needed. The as-grown crystals had a black color and a rectangular shape.

The samples obtained were characterized by means of neutron diffraction and fluorescent analysis. The chemical composition was determined based on the relation of $K_\alpha La$ and $K_\alpha Ba$ lines of secondary characteristic radiation spectra. The perturbation of the main elements were realized by ^{241}Am ($\gamma = 59.54$ keV) radioisotope source. The X-ray spectrometer provided by Si(Li)-semiconductor detector was used to register the secondary characteristic radiation with 200 eV accuracy at 5.95 keV line from ^{55}Fe radioisotope source.

The spin wave dispersion relations were measured using the thermal triple-axis instruments at the NIST Center for Neutron Research. Resistivity measurements of the as-grown crystals were made by standard four-probe method using silver paste for low resistance contacts preparing. Magnetic transition temperatures were determined by measuring AC-magnetic susceptibility and by neutron diffraction.

3. Stability area of $La_{1-x}Ba_xMnO_3$ phase in B_2O_3–BaO–BaF_2 solvent

A series of $LaMnO_3$–B_2O_3–BaO–BaF_2 system parameters: solubility isotherms, saturation temperature versus BaF_2 content in the flux melt, and the evaporation kinetics at various BaF_2 concentrations have been studied and found to agree qualitatively with the $EuFeO_3$–B_2O_3–BaO–BaF_2 system properties investigated earlier [9]. As we have expected weight losses of volatile components increase with BaF_2 concentration in the flux melt and temperature rising. The pseudoternary phase diagram of the system shows the range of flux-melt compositions that allowed us to grow $La_{1-x}Ba_xMnO_3$ crystals as a primary phase in the temperature interval 950–1250°C (Fig. 1a). We have to state that the primary crystallization area is of a very tentative character because high volatile components are beyond calculation. However, we have enough data to argue that a dashed AB curve belongs to the upper boundary, while more

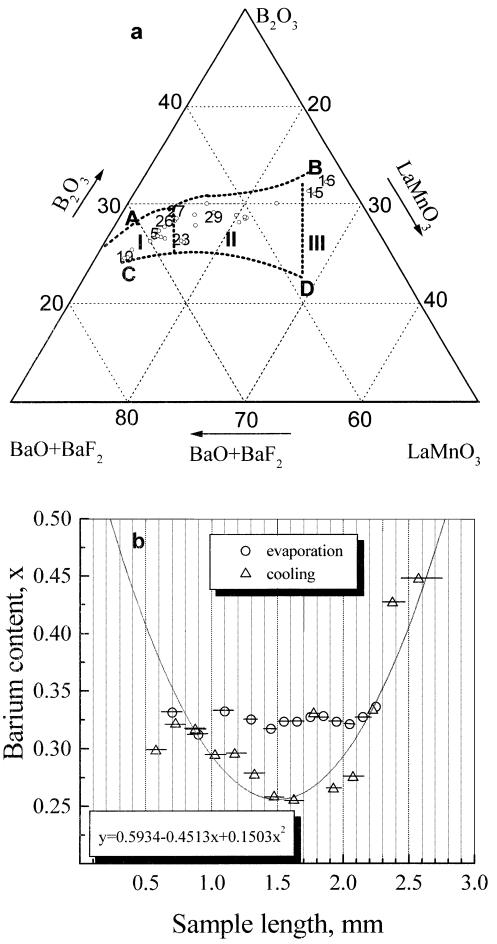

Fig. 1. Data of $La_{1-x}Ba_xMnO_3$ crystals flux growth: (a) three ranges of flux-melt compositions on the $LaMnO_3$–B_2O_3–BaO–BaF_2 phase diagram; (b) layer by layer analysis of Ba content in two crystals were grown either by flux slow cooling or by evaporation at constant temperature.

tentative CD curve corresponds to a lower border of the manganite phase stability range. Particularly, lanthanum borates and $La_{1-x}Ba_xMnO_3$ co-crystallization was found as a result of growth run using the flux melts corresponding to 26 and 27 points in the phase diagram. Despite extensive flux weight loss, a three week growth run from flux composition labeled as 19 and 23 provides large volume crystals with Ba content $x = 0.43$ and $\frac{1}{3}$ correspondingly. However, flux instability caused drastic changes of growth conditions when flux composition passed down through the CD phase boundary, resulting in a boosted growth rate of lanthanum borates and consequent reduction in manganite crystal growth. A distinguish gradation of Ba concentration was registered for $La_{1-x}Ba_xMnO_3$ crystals grown from the same composition of flux melt, but at different temperatures (degree of flux supersaturation) to confirm the inverse temperature dependence of Ba distribution coefficient in the (La,Ba)MnO_3–B_2O_3–BaO–BaF_2 system. Fig. 1b shows data of a layer by layer X-ray fluorescent analysis of Ba content in two $La_{1-x}Ba_xMnO_3$ crystals which were grown either by flux supersaturation with slow cooling or by evaporation at constant temperature. In this case a parabolic-like dependence of Ba content in layers through the sample length was found. From the other side, one can see a good

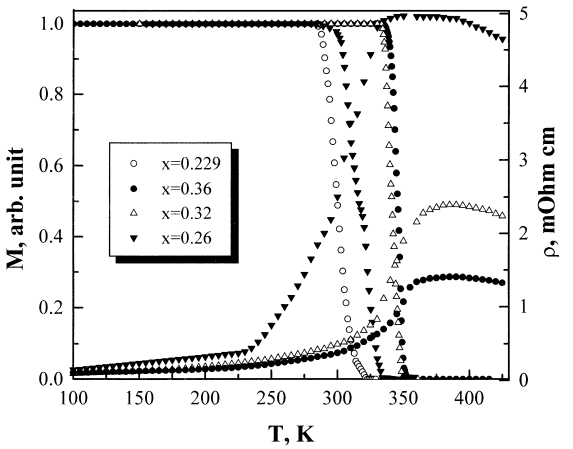

Fig. 2. Resistivity and AC-susceptibility of the $La_{1-x}Ba_xMnO_3$ crystals depending on Ba content.

~2% homogeneity of Ba distribution in the crystal has grown by the last technique. The result can be easily understood by taking into account the inverse temperature dependence of the Ba content in probe samples that have been grown at different temperatures by evaporation technique. For this reason a technique of evaporation under constant or at very slow temperature sweep was used to grow neutron-sized crystals of $La_{1-x}Ba_xMnO_3$ ($0.2 < x < 0.5$) with a good Ba homogeneity in volume (see Table 1). The flux compositions corresponding to I, II and III regions in the quasi ternary phase diagram (Fig. 1a) were used to grow $x > 0.35$, $x = 1/3$, and $x < 0.25$ crystals, respectively.

4. Spin dynamics, magnetic susceptibility and electrical resistivity of $La_{1-x}Ba_xMnO_3$

Fig. 2 presents the AC-susceptibility and electrical resistivity data of the as-grown $La_{1-x}Ba_xMnO_3$ crystals depending on Ba content. For all the samples one can see the metal–insulator phase transition takes place at a peak temperature (T_p) rather above the ferromagnetic ordering temperature (T_c) as well as the peak magnitude of magnetoresistance ~50% at applied field up to 2 T in the vicinity of T_c. The result differs from the data presented for a ceramic sample with the same composition, where $T_c = T_p$ [10].

Neutron scattering has been used to study the spin dynamics of $La_{0.68}Ba_{0.32}MnO_3$. In the long-wavelength regime the spin-wave dispersion relations are found to be isotropic in wave vector q, with a gapless excitation spectrum indicative of an ideal isotropic ferromagnet, as has been found for most of the doped manganite systems in the ferromagnetic regime [11–14]. Fig. 3 shows the spin waves to the zone boundary in the [1 0 0] direction, with a maximum energy of 30 meV at low temperatures. The spin waves soften with increasing temperature in the usual manner. At small wave vectors we also find that the spin stiffness parameter $D(T)$ (defined by $E = D(T)q^2$) obeys a power law in reduced temperature T/T_c (not shown). The ordering temperature as determined by Bragg

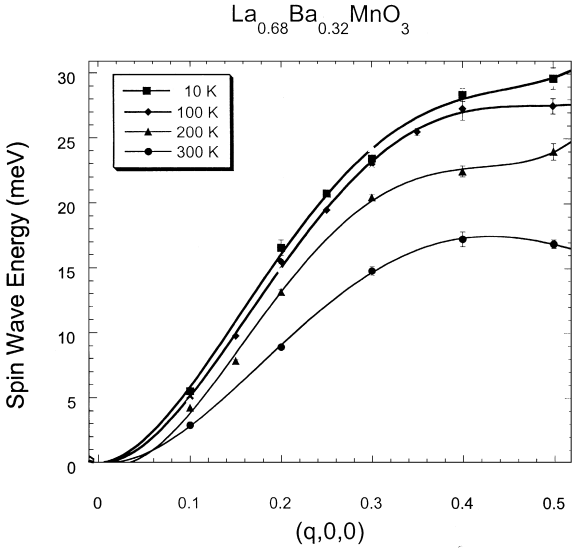

Fig. 3. Spin-wave dispersion relation along the [1,0,0] direction of $La_{0.68}Ba_{0.32}MnO_3$ as a function of temperature.

reflection of neutrons is 336 ± 1 K, which is in excellent agreement with bulk magnetization measurements. In the ferromagnetic state an anomalous spin diffusion component develops in the fluctuation spectrum as $T \to T_p$ for polycrystalline sample, which is attributed to the spin component of the polaron in these materials. In the single crystals this scattering is weak in the ordered phase because $T_P > T_C$. Then, as the ferromagnetic behavior begins to develop, the charge ordering melts and the system becomes metallic. Our data suggest that the development of the polaron component in the fluctuation spectra of $La_{1-x}Ba_xMnO_3$ is directly correlated with T_p.

5. Conclusions

The primary crystallization area of Ba-doped lanthanum manganites on the corresponding pseudoternary phase diagram was determined. The technique of evaporation under constant or at very slow temperature sweep was used to grow with a seed neutron-sized crystals of $La_{1-x}Ba_xMnO_3$ ($0.2 < x < 0.5$), which reveal a good Ba homogeneity in volume. In contrast to ceramic samples, where $T_c = T_p$, for all single crystals the metal–insulator phase transition takes place at a peak temperature rather above the ferromagnetic ordering temperature. For this reason in the single crystals the spin component of the polaron is weak in the ordered phase.

Acknowledgements

The work in Minsk was supported in part by the INTAS under grants No 96-0410 and 97-1371. Research at the University of Maryland was supported by the US NSF, DMR97-01339, and MRSEC, DMR 96-32521.

References

[1] G.H. Jonker, J.H. Van Santen, Physica 16 (1950) 337.
[2] S. Jin, T.H. Tiefel, M. McCormack et al., Science 264 (1994) 413.
[3] D.W. Visser, A.P. Ramirez, M.A. Subramanian, Phys. Rev. Lett. 78 (1997) 3947.
[4] M. Nevrjiva, E. Pollert, Cryst. Res. Technol. 19 (1984) 147.
[5] J.Z. Liu, I.C. Chang, S. Irons et al., Appl. Phys. Lett. 66 (1995) 3218.
[6] Y. Tomioka, A. Asamitsu, Y. Moritomo et al., Phys. Rev. Lett. 74 (1995) 5108.
[7] Y. Kuwahara, Y. Tomioka, A. Asamitsu et al., Science 270 (1995) 961.
[8] A.M. Balbashov, S.G. Karabashev, Ya.M. Mukovskiy et al., J. Crystal Growth 167 (1996) 365.
[9] S.N. Barilo, A.P. Ges, S.A. Guretskii et al., J. Crystal Growth 108 (1991) 309.
[10] H.L. Ju, J. Gopalakrishnan, J.L. Peng et al., Phys. Rev. B 51 (1995) 6143.
[11] J.W. Lynn, R.W. Erwin, J.A. Borchers et al., Phys. Rev. Lett. 76 (1996) 4046.
[12] J.W. Lynn, Int. J. Mod. Phys. 12 (1998) 3355.
[13] L. Vasiliu-Doloc, J.W. Lynn, A.H. Moudden et al., Phys. Rev. B 58 (1998) 14913.
[14] J.W. Lynn, L. Vasiliu-Doloc, M.A. Subramanian, Phys. Rev. Lett. 80 (1998) 4582.